



# Study on the Heat Transfer Characteristics of a Vapor Chamber without Micro-channel for Cooling an Electronic Component

Songkran Wiriyasart and Paisarn Naphon

Thermo-Fluids and Heat transfer Enhancement Lab TFHT),  
Department of Mechanical Engineering, Faculty of Engineering, Srinakharinwirot University

## Correspondence:

Songkran Wiriyasart  
Department of Mechanical Engineering,  
Faculty of Engineering, Srinakharinwirot  
University, 63 Rangsit-Nakhon Nayok  
Rd., Ongkharak, Nakhon Nayok, 26120  
E-mail: songkran.w@th.fujikura.com

## Abstract

*Numerical results on the thermal performance of vapor chamber without micro-channel for cooling computer processing unit (CPU) are presented. The vapor chamber is an advanced cooling heat spreader for cooling CPUs in personal computers and work stations. The results obtained from the model are compared with those from the measured data. The mathematical model of the vapor chamber in this study is a two-phase closed chamber with wick sheet and a wick column. By solving the equations of continuity, momentum, and energy numerically, the pressure and temperature distributions inside the vapor chamber are presented. In the experiment, the CPU is replaced by a heater as the heat source, with power input of 80 W. The experimental tests are carried out, and good agreement is obtained with the numerical results. These numerical results are useful for the design to improve thermal performance of the vapor chamber, and also diminished the expense and time of the real test.*

*Keywords: Vapor Chamber, Micro-Channel, Liquid cooling,  
Computer Processing Unit;*

## 1. Introduction

In recent years, CPU cooling techniques have been developed to handle increasing heat load. In general, a heat sink is used for cooling a CPU and electronic devices. However, because the heat generated by the CPU is more than the capacity of the cooling equipment currently in use, it is necessary to develop cooling efficiency that can accommodate the heat load at the actual CPU. Two phase heat spreading devices such as vapor chambers (phase change) have been developed and proven to be among the most efficient passive cooling devices for cooling electronic components especially CPUs of personal computers, laptops, servers, data centers etc., As compared to other cooling devices such as fans, thermoelectric modules, liquid pump loop devices, the vapor chamber cooling technique has simple structures, has no moving parts, and does not use electricity. Numerical and experimental analysis of the thermal performance of the heat sink and vapor chamber as cooling devices have been widely examined by researchers. Attia and Assal [1] studied the thermal performance of a vapor chamber with water and methyl alcohol at different charge ratios. Elnaggar et al. [2,3] experimentally and numerically investigated the performance of a finned U-shape heat pipe, and characterized the working fluid in a vertically oriented twin U-shape heat pipe. Hassan and Harmand [4] considered the three-dimensional transient

model for a vapor chamber and the effect of nano fluids on its performance. Hong and Cheng [5] characterized the water evaporation/boiling on copper particle sintered porous wick, determining the performance of a vapor chamber. Ji and Xu [6] studied an extended vapor chamber, consisting of an evaporator part and an extended condenser part. Ju and Kaviany [7] experimentally studied advanced evaporator wicks and thin planar vapor chambers. Li et al. [8] investigated the effects of a shield on the thermal and hydraulic characteristics of plate-fin vapor chamber heat sinks. Naphon et al. [9,10] experimentally studied the thermal cooling of vapor chamber for cooling CPUs and HDDs of PCs. Tsai and Kang [11] experimentally studied the thermal resistance in a vapor chamber heat spreader. Weibel and Garimella [12] investigated the capillary-fed boiling of water from porous sintered powder wicks used in emerging highly effective-conductivity vapor. Wong et al. [13] experimentally studied the vapor chamber performance with a working fluid of water, methanol, or acetone.

The purpose of this paper is to study the thermal performance of the vapor chamber without micro-channel for cooling a computer processing unit. The predicted results are verified with the measured data.

## 2. Experimental Apparatus and Method

The test loop consists of a wind tunnel, a Vapor chamber cooling system, and a data acquisition system. The vapor chamber cooling system consists of the vapor chamber, heat sink unit, and axial fan wind tunnel unit. In an experiment, the CPU is replaced by 2 heaters inside a copper block as the heat source with power input of 80 W by a power supply. The wind tunnel is generates an air flow rate through the fin channel of the vapor chamber of 12 CFM. The schematic diagram of the vapor chamber unit is shown in Fig. 1. The vapor chamber is fabricated from copper plates, which consists of a bottom copper plate, wick sheet, sinter column, and the top copper plate. The wick sheet and the sinter column are fabricated from copper powder. The bottom copper plate is the evaporator section that may be mounted on an electrical heater to absorb the generated heat, and the other is the condenser section, which heat is transferred to the heat sink and air, respectively. In order to minimize thermal resistance between the electrical-vapor chambers and vapor chamber-heat sink unit, a thin film of high thermal conductivity grease is applied at their junction interface. The working fluid (de-ionized water) is evaporated on the heated side and condensed on the cooling side and then returns to the evaporator section under gravity. Type T copper-constantan thermocouples with an accuracy of 0.1% of full scale are employed to measure the temperatures. A groove within the chamber walls is machined and high conductivity cement is utilized to embed the thermocouples within the chamber wall. All thermocouples are pre-calibrated with a dry box temperature calibrator. A vapor chamber without micro-channel on the evaporator section is tested in the present study. Type T copper-constantan thermocouples with an accuracy of 0.1% of full scale are employed to measure the temperatures. Four type T copper-constantan thermocouples are applied to measure the vapor chamber temperature. One thermocouple is applied to observe the ambient temperature and two thermocouples measure the air inlet and out-let temperature. A groove of 1x1 mm within the heater surface is machined and high conductivity cement is utilized to embed the thermocouples within the heater surface that touch the vapor chamber. All thermocouples are pre-calibrated with a dry box temperature calibrator.

The vapor chamber without micro-channel on the evaporator section is tested in the present study. Type T copper-constantan thermocouples with an accuracy of 0.1% of full scale are employed to measure the temperatures. Four type T copper-constantan thermocouples are applied to measure the vapor chamber temperature. One thermocouple is applied to observe the ambient temperature. Two thermocouples are used to measure the air inlet and out-let temperature. A groove of 1x1 mm within the heater surface is machined and high conductivity cement is utilized to embed the thermocouples within the heater surface that touched to the vapor chamber. All thermocouples are pre-calibrated with a dry box temperature calibrator. The temperatures at each position were recorded in a period of 15 min or until steady state. Data collection was carried out using a data acquisition system.

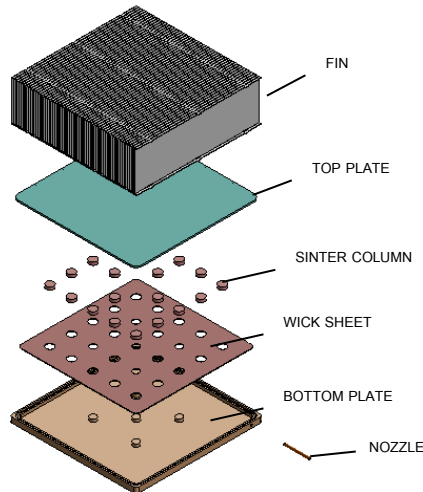


**Fig.1.** Schematic diagram of the vapor chamber.

Based on the computational domains as shown in Fig. 2, a 3D transient thermal model coupled with a 3D transient hydrodynamic model is used to solve the model. The transient thermal and hydrodynamic models are used to calculate the vapor chamber temperature and pressure. All free wall surfaces are assumed to be adiabatic, and the fluid flow is assumed to be laminar and incompressible, and the effect of gravity is neglected. The Transient model is based on the numerical solution of the governing equations of the mass, momentum, and energy in the two phases and the liquid/vapor interface [2][3][4].

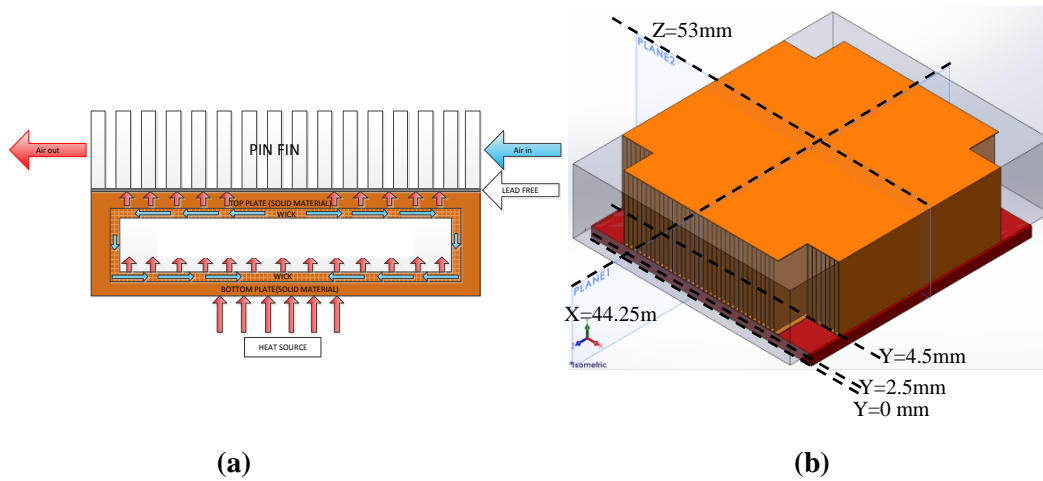


**Fig.2.** Schematic diagram of the computational.

The differential mass equation is:

$$\frac{\partial u_1}{\partial x} + \frac{\partial v_1}{\partial y} + \frac{\partial w_1}{\partial z} = 0 \tag{1}$$

The liquid flow through the wick is governed by the momentum equations:

$$\frac{\rho}{\varepsilon} \left( \frac{\partial u_1}{\partial t} + u_1 \frac{\partial u_1}{\partial x} + v_1 \frac{\partial u_1}{\partial y} + w_1 \frac{\partial u_1}{\partial z} \right) = -\frac{\partial p_1}{\partial x} - \frac{\mu_1}{K} u_1 + \frac{\mu_1}{\varepsilon} \left[ \frac{\partial^2 u_1}{\partial x^2} + \frac{\partial^2 u_1}{\partial y^2} + \frac{\partial^2 u_1}{\partial z^2} \right] - \frac{C_E}{K^{0.5}} |V|V \quad (2)$$

$$\frac{\rho}{\varepsilon} \left( \frac{\partial v_1}{\partial t} + u_1 \frac{\partial v_1}{\partial x} + v_1 \frac{\partial v_1}{\partial y} + w_1 \frac{\partial v_1}{\partial z} \right) = -\frac{\partial p_1}{\partial y} - \frac{\mu_1}{K} v_1 + \frac{\mu_1}{\varepsilon} \left[ \frac{\partial^2 v_1}{\partial x^2} + \frac{\partial^2 v_1}{\partial y^2} + \frac{\partial^2 v_1}{\partial z^2} \right] - \frac{C_E}{K^{0.5}} |V|V \quad (3)$$

$$\frac{\rho}{\varepsilon} \left( \frac{\partial w_1}{\partial t} + u_1 \frac{\partial w_1}{\partial x} + v_1 \frac{\partial w_1}{\partial y} + w_1 \frac{\partial w_1}{\partial z} \right) = -\frac{\partial p_1}{\partial z} - \frac{\mu_1}{K} w_1 + \frac{\mu_1}{\varepsilon} \left[ \frac{\partial^2 w_1}{\partial x^2} + \frac{\partial^2 w_1}{\partial y^2} + \frac{\partial^2 w_1}{\partial z^2} \right] - \frac{C_E}{K^{0.5}} |V|V \quad (4)$$

For the vapor core, the mass conservation equation is:

$$\frac{\partial u_V}{\partial x} + \frac{\partial v_V}{\partial y} + \frac{\partial w_V}{\partial z} = 0 \quad (5)$$

The vapor flow through the vapor region is governed by the momentum equations:

$$\rho_V \left( \frac{\partial u_V}{\partial t} + u_V \frac{\partial u_V}{\partial x} + v_V \frac{\partial u_V}{\partial y} + w_V \frac{\partial u_V}{\partial z} \right) = -\frac{\partial p_V}{\partial x} + \mu_V \left[ \frac{\partial^2 u_V}{\partial x^2} + \frac{\partial^2 u_V}{\partial y^2} + \frac{\partial^2 u_V}{\partial z^2} \right] \quad (6)$$

$$\rho_V \left( \frac{\partial v_V}{\partial t} + u_V \frac{\partial v_V}{\partial x} + v_V \frac{\partial v_V}{\partial y} + w_V \frac{\partial v_V}{\partial z} \right) = -\frac{\partial p_V}{\partial y} + \mu_V \left[ \frac{\partial^2 v_V}{\partial x^2} + \frac{\partial^2 v_V}{\partial y^2} + \frac{\partial^2 v_V}{\partial z^2} \right] \quad (7)$$

$$\rho_V \left( \frac{\partial w_V}{\partial t} + u_V \frac{\partial w_V}{\partial x} + v_V \frac{\partial w_V}{\partial y} + w_V \frac{\partial w_V}{\partial z} \right) = -\frac{\partial p_V}{\partial z} + \mu_V \left[ \frac{\partial^2 w_V}{\partial x^2} + \frac{\partial^2 w_V}{\partial y^2} + \frac{\partial^2 w_V}{\partial z^2} \right] \quad (8)$$

The heat transfer in the vapor chamber wall is expressed with the energy equation [4]:

$$(\rho C)_w \frac{\partial T}{\partial t} = \lambda_w \left( \frac{\partial^2 T}{\partial x^2} + \frac{\partial^2 T}{\partial y^2} + \frac{\partial^2 T}{\partial z^2} \right) \quad (9)$$

In the wick region, the energy equation is:

$$(\rho C)_{wi} \left( \frac{\partial T}{\partial t} + u_1 \frac{\partial T}{\partial x} + v_1 \frac{\partial T}{\partial y} + w_1 \frac{\partial T}{\partial z} \right) = \lambda_w \left( \frac{\partial^2 T}{\partial x^2} + \frac{\partial^2 T}{\partial y^2} + \frac{\partial^2 T}{\partial z^2} \right) \quad (10)$$

In the vapor region, the energy equation is:

$$(\rho C)_v \left( \frac{\partial T}{\partial t} + u_V \frac{\partial T}{\partial x} + v_V \frac{\partial T}{\partial y} + w_V \frac{\partial T}{\partial z} \right) = \lambda_V \left( \frac{\partial^2 T}{\partial x^2} + \frac{\partial^2 T}{\partial y^2} + \frac{\partial^2 T}{\partial z^2} \right) \quad (11)$$

Where  $C_E$  is Ergun coefficient;  $C$  is specific heat capacity;  $K$  is permeability;  $p$  is pressure;  $p_c$  is capillary pressure;  $q$  is heat flux density;  $R$  is gas constant;  $t$  is time;  $T$  is temperature;  $u$ ,  $v$ , and  $w$  are velocity;  $V$  is total velocity;  $x$ ,  $y$ ,  $z$  are coordinates.



The computational domain used in the present study is shown in Fig. 2. In order to assess the accuracy of these computations, computational grids with  $7.3 \times 10^5$ ,  $8.5 \times 10^5$ ,  $9.2 \times 10^5$  grids are used to test the grid independence of the solution. The grid independence test indicated that the grid systems of  $8.5 \times 10^5$  ensure a satisfactory solution. The boundary conditions of the numerical analysis are shown in Table 1. Based on the results shown in Table 2, a computational grid with  $8.5 \times 10^5$  is employed throughout the computation in the present study. The numerical study is simulated under constant average heat flux. The commercial program ANSYS/FLUENT has been employed as the numerical solver.

#### 4. Results and discussion

In the practical applications, the heat sink is attached to a heat generation source such as a CPU to receive heat and dissipate it by fluid flow through the heat sink. The wind tunnel generates the air flow rate through the fin channel of the vapor chamber of 12 CFM. In an experiment, the CPU is replaced by 2 heaters inside a copper block as the heat source with power input of 80 W by a power supplier. Therefore, the numerical study is simulated under average constant heat flux on the rear face of the heat sink. Table 2 also shows the comparison between the predicted heat source temperatures with the measured data. It is found that the maximum relative different is within 1.4%, indicating that the chosen computation grid ( $8.3 \times 10^5$ ) produces acceptable results.

**Table 1.** Boundary conditions of the numerical analysis used in the present study.

Problem Setup	Major	Minor
General	Model	3D
	Time	Transient
	Gravity	Y Axis-9.81m/s <sup>2</sup>
Models	Multiphase	Mixture
	Energy	Used
	Viscous	Laminar
Boundary conditions	Inlet	Velocity inlet, $T_{air\ in}$ , Volume fraction=1
	Wall	Standard wall function, $T_{wall}$ (constant), no slip condition
	Outlet	Pressure outlet, Back flow volume fraction=1
	Wall hot	Heat Flux
	Interfaces	Interface
Solution Methods	Scheme	Simple
	Spatial Discretization	First Order
	Transient Formulation	First Order Implicit

**Table 2.** Comparison between the measured heat source temperature and the predicted results.

Predicted results (°C)	Measured data (°C)	% Difference
46.15	45.50	1.4

The vapor chamber is a cavity with small thickness that is filled with the working fluids and is fitted between the top of the heat source and the bottom of the heat sink. For electronic cooling with a vapor chamber, the bottom copper plate is the evaporator section that may be mounted on the electronic components to absorb generated heat, and the other is the condenser section, in which heat is transferred to the heat sink and air, respectively. The liquid returns from the evaporator to the condenser through a capillary structure composed of microgrooves, meshes, and sintered powder wicks. The numerical

results on the thermal performance of vapor chamber without mini-channel for cooling a computer processing unit (CPU) are presented. The vapor chamber for this test was optimized for a water charge ratio of around 28% by volume of the vapor chamber, excluding porosity of sinter column and wick sheet.

The three dimensional temperature distribution throughout the vapor chamber at  $Y=0$  mm,  $Y=2.5$  mm, and  $Y=4.5$  mm is shown in Fig. 3. It can be seen that the maximum heat source temperature is located at the center of the bottom surface of the evaporator at the heat source input. This heat is transferred through the sinter column and the wick sheet to the condenser plate and the heat sink, respectively. Therefore, the temperature distribution at the condenser surface and heat sink are more uniform as shown in Figs. 3 (b) and (c), respectively. In addition, there is reasonable agreement between the measured data and the predicted results. It can be seen that the temperature distribution from heat source through sinter column and wick sheet to the heat sink dropped around  $3^{\circ}\text{C}$ . The temperature distribution at  $X=53$  and  $Y=44.25$  are shown in Fig.4 (a) and (b), respectively. It is shown that the maximum heat source temperature at the center of the bottom surface of the evaporator at the heat source input. The flow pattern of the air at the inlet plenum has a significant effect on the heat transfer of the vapor chamber at the fin area, as shown in Fig 4 (a). After the fluid flows into the vapor inlet in the normal direction, it can be seen that temperatures at the inlet is lower than that of the outlet. The temperature at the outlet of the fin is the highest.

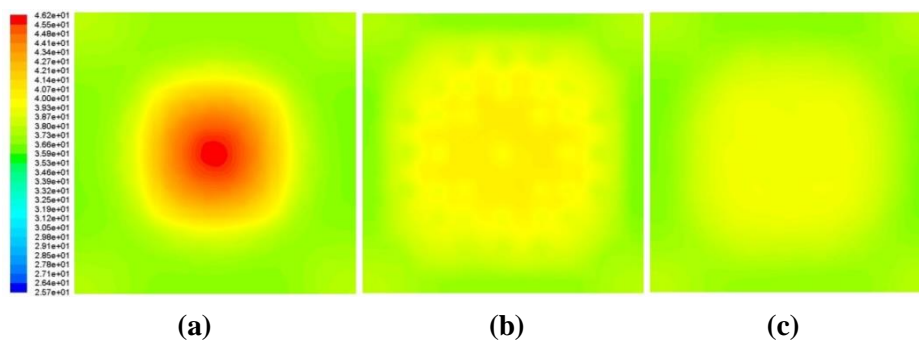


**Fig. 3.** The three dimension temperature distribution throughout the vapor chamber at (a)  $Y=0$  mm, (b)  $Y=2.5$  mm, (c)  $Y=4.5$  mm.

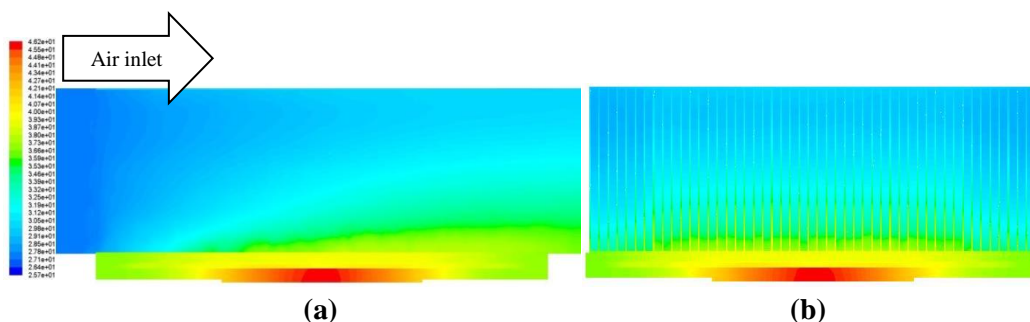


**Fig. 4.** three dimension temperature distribution throughout the vapor chamber at  $X=53$ ,  $Y=44.25$ .

The temperature distribution at  $Y=44.25$  is shown in Fig 4 (b). It can be seen that the highest temperatures occur at the center of the heat source and fin. Due to the shorter fins on the left and right hand sides (Fig. 2), the temperature distributions in these zones are lower than those in the other zones.

#### 4. Conclusion

Numerical results on the thermal performance of a vapor chamber without micro-channel for cooling a computer processing unit (CPU) are presented. Vapor chamber applications for electronic



cooling have many advantages as compared to other cooling devices such as fans, thermoelectric modules and liquid pump loop devices. It has a simple structure, no moving parts, and does not use electricity. The results obtained from the model are compared with those from the measured data. The experimental tests are carried out and good agreement is obtained with the numerical results. These numerical results are useful for the design to improvement thermal performance of the vapor chamber and also diminished the expense and time of a real test.

## 5. Acknowledgments

The authors would like to express their appreciation to the Excellent Center for Sustainable Engineering (ECSE) of the Srinakharinwirot University (SWU).

## References

- [1] Attia, A.A. and EI-Assal, B., Experimental investigation of vapor chamber with different working fluids at different charge ratios, *Ain Shams Engineering Journal*, Vol. 3, No. 3, pp. 289-297, 2012.
- [2] Elnaggar, M. Abdullah, M.Z. Abdul, M., Experimental analysis and FEM simulation of finned U-shape multi heat pipe for desktop PC cooling, *Energy Conversion and Manage*, Vol, 52, No. 8-9, pp. 2937-2944, 2011.
- [3] Elnaggar, M. Abdullah, M.Z. Abdul, M., Characterization of working fluid in vertically mounted finned U-shape twin heat pipe for electronic cooling, *Energy Conversion and Management*, Vol. 62, pp. 31-39, 2012.
- [4] Hassan, H. and Harmand, S., 3D transient model of vapour chamber: Effect of nanofluids on its performance, *Applied Thermal Engineering*. Vol. 51, No. 1-2, pp. 1191-1201, 2013.
- [5] Hong, F.J. Cheng, P. H. Wu, Y. Z. Sun, Z., Evaporation/boiling heat transfer on capillary feed copper particle sintered porous wick at reduced pressure, *International Journal of Heat and Mass Transfer*, Vol. 63, pp. 389-400, 2013.
- [6] Ji, X. Xu, J. Abanda, A.M. Xue, Q., A vapor chamber using extended condenser concept for ultra-high heat flux and large heater area, *International Journal of Heat and Mass Transfer*, Vol. 55, No. 17-18, pp. 4908-4913, 2012.
- [7] Ju, Y.S. Kaviany, M. Nam, Y. Sharratt, S. Hwang, G.S. Catton, I. Fleming, E. Dussinger, P., Planar vapor chamber with hybrid evaporator wicks for the thermal management of high-heat-flux and high-power optoelectronic devices, *International Journal of Heat and Mass Transfer*, Vol. 60, pp. 163-169, 2013.
- [8] Li, H.Y. Chiang, M.H. Lee, C.I. Yang, W.J., Thermal performance of plate-fin vapor chamber heat sinks, *International Journal of Heat Mass Transfer*, Vol. 37, No.7, pp. 731-738, 2010.
- [9] Naphon, P. Wongwises, S. Wiriyasart, S., On the thermal cooling of central processing unit of the PCs with vapor chamber, *International Communication in Heat and Mass Transfer*, Vol. 39, No. 8, pp. 1165-1168, 2012.
- [10] Naphon, P. Wongwises, S. Wiriyasart. S., Application of two-phase vapor chamber technique for hard disk drive cooling of PCs, *International Communication in Heat and Mass Transfer*, Vol. 40, pp. 32-35, 2013.
- [11] Tsai, M.C. Kang, S.W. Paiva, K.V., Experimental studies of thermal resistance in a vapor chamber heat spreader, *Applied Thermal Engineering*, Vol. 56, No. 1-2, pp. 38-44, 2013.
- [12] Weibel J.A. and Garimella, S.V., Visualization of vapor formation regimes during capillary-fed boiling in sintered-powder heat pipe wicks, *International Journal of Heat and Mass Transfer*, Vol. 55, No. 13-14, pp. 3498-3510, 2012.
- [13] Wong, S.C. Huang, S.F. Hsieh, K.C., Performance tests on a novel vapor chamber, *Applied Thermal Engineering*, Vol. 31, No. 10, pp. 1757-1762, 2011.